Iraqi Journal of Science, 2020, Vol. 61, No.2, pp: 266-276
DOI: 10.24996/ijs.2020.61.2.9

ISSN: 0067-2904

Green Synthesis and the Study of Some Physical Properties of MgO Nanoparticles and Their Antibacterial Activity

Rand Ali[*1], Zainab J. Shanan[1], Ghada Muhammad Saleh[2], Quraysh Abass[3]
[1]Department of Physics, College of Science for Women, University of Baghdad.
[2]Department of Biology, College of Science, University of Baghdad
[3]Chemical and Petrochemical Research Center [3], Iraqi Ministry of Industry and Minerals, Iraq

Received: 10/7/ 2019 Accepted: 28/ 8/2019

Abstract

Magnesium oxide nanoparticles (MgO NPs) were synthesized by a green method using the peels *of Persimmon* extract as the reducing agent , magnesium nitrate, and NaOH. This method is eco-friendly and non-toxic. In this study, an ultrasound device was used to reduce the particle size, with the impact on the energy gap was set at the beginning at 5.39 eV and then turned to 4.10 eV. The morphological analysis using atomic force microscopy (AFM) showed that the grain size for MgO NPs was 67.70 nm which became 42.33 nm after the use of the ultrasound. The shape of the particles was almost spherical and became cylindrical. In addition the Field-Emission Scanning Electron Microscopy (FESEM) analysis showed that the average particle size was reduced and the spherical shape was changed into cylindrical flakes. The antibacterial activity of MgO Nps was measured against both gram positive and negative bacteria (*Staphylococcus aureus and Escherichia coli*, respectively) for both the synthesized and the scaled-down particles by the ultrasonic. MgO NPs showed an efficacy at a minimum inhibitory concentration (MIC) of 500 µg/ml, with the better effect being observed after the ultrasonic treatment of the MgO NPs.

Keywords: Magnesium oxide nanoparticle, Green method, Atomic Force Microscopy, Bacteria, Ultrasonic processor, and minimum inhibitory concentration (MIC).

التوليف الاخضر ودراسة بعض الخصائص الفيزيائية للجزيئات النانوية لل MgO وفعاليتها المضادة للبكتيريا

رند علي[*1]، زينب جاسم[1]، غادة محمد صالح[2] ، قريش عباس[3]
[1]قسم الفيزياء ، كلية العلوم للبنات ، جامعة بغداد.
[2]قسم الأحياء ، كلية العلوم ، جامعة بغداد.
[3]مركز البحوث الكيميائية والبتروكيماوية ، وزارة الصناعة والمعادن العراقية ، العراق.

الخلاصة

تم تصنيع جزيئات أكسيد ا المغنسيوم النانوية (MgO NPs) بطريقة الخضراء باستخدام مستخلص قشور البرسيمون كعامل اختزال ، نترات المغنسيوم و NaOH. هذه الطريقة صديقة للبيئة وغير سامة. في هذه

*Email: rand_ali90@yahoo.com

الدراسة ، تم استخدام جهاز الموجات فوق الصوتية لتقليل حجم الجسيمات وكان التأثير على فجوة الطاقة في بداية 5.39 فولت وتم تحويله إلى 4.10 فولت. وأظهر التحليل المورفولوجي باستخدام مجهر القوة الذرية (AFM) أن حجم الدقائق لل MgO NPs كان 67.70 نانومتر وأصبح 42.33 نانومتر بعد استخدام الموجات فوق الصوتية ، وكان شكل الجزيئات كروية تقريبا وأصبح أسطواني. بالإضافة إلى ذلك ، أظهر تحليل المجهر المسح الضوئي للانبعاثات الالكترونية (FESEM) أن متوسط حجم الدقائق قد انخفض وأن الشكل الكروي يتحول إلى رقائق أسطوانية. تم قياس الفعالية المضادة للبكتيريا لـ MgO Nps مقابل كل من البكتيريا الموجبة والسالبة (*Staphylococcus aureus*) و (*Escherichia coli*)على التوالي لكل من الجسيمات المصنعة والمصغرة بواسطة الموجات فوق الصوتية ، وأظهرت MgO NPs ان التركيز المثبط الادنى (MIC) في 500 ميكروغرام / مل مع تأثير أفضل لل MgO NPsالمعاملة بالموجات فوق الصوتية.

Introduction

Modern studies show that the metal oxide and metal nanomaterials demonstrate noticeable positive results in many fields [1-4]. Metal oxide nanoparticles attracted attention due to their increased use in various fields such as cosmetics, electronics, material sciences, catalysis, environment, energy and Biomedicine [5, 6]. MgO nanoparticles have interesting applications in microelectronics, diagnostics, and biomolecular detection. Green synthesis of MgO nanoparticles was carried out using the peels of *Persimmon* extract for the predominantly ecofriendly processing with remarkable novel technologies [7]. MgO is considered as a safe material for humans and animals. There are several methods for the synthesis of nano-sized MgO particles, including laser deposition, sol- gel , hydrothermal synthesis , aerosol synthesis, and chemical gas deposition [8, 9]. The toxicity of metal oxide nanoparticals and their antimicrobial activity are attracting very much research. Among such oxides is the MgO with its low cost and eco-friendly properties, while its toxicity is conferred by the production of reactive oxygen species (ROS) [10]. MgO NPs were shown to have antimicrobial activities against different microbial species, especially bacteria [11], which needs to be further investigated on different levels. Persimmon is also named kaki, which has been cultivated in Japan for several centuries. It is believed to have originated in southern China. The fruits of kaki are astringent until fully ripe. Persimmon contains many biologically active compounds, such as tannins, carotenoids, flavonoids, steroids, naphthoquinones, terpenoids, sugars, minerals, amino acids, and lipids [12]. In general, the peel was seen as a waste matter, although recent studies have shown that peel contains biologically and nutritionally beneficial compounds [13]. Ultrasound is a very active processing method in the application and generation of nano-size materials. In general, ultrasonic cavitation in liquids may cause fast and complete degassing; it accelerates chemical reactions by facilitating the mixing of reactants; it enhances polymerization and depolymerization reactions by temporarily dispersing aggregates or by permanently breaking chemical bonds in polymeric chains [14]. Ultrasound is applied in a vast range of physical, biological and chemical processes. Emulsifying and dispersing are examples of physical processes. Most of the uses of high-intensity ultrasound are based on the cavitation effects [15]. The nanoparticles and mini nanoparticles of MgO synthesized using ultrasonic processor were analyzed as related to their antibacterial activities.

Materials and methods

Green method of synthesis of MgO NPs

Preparation of hot aqueous extracts of the *Persimmon* peels

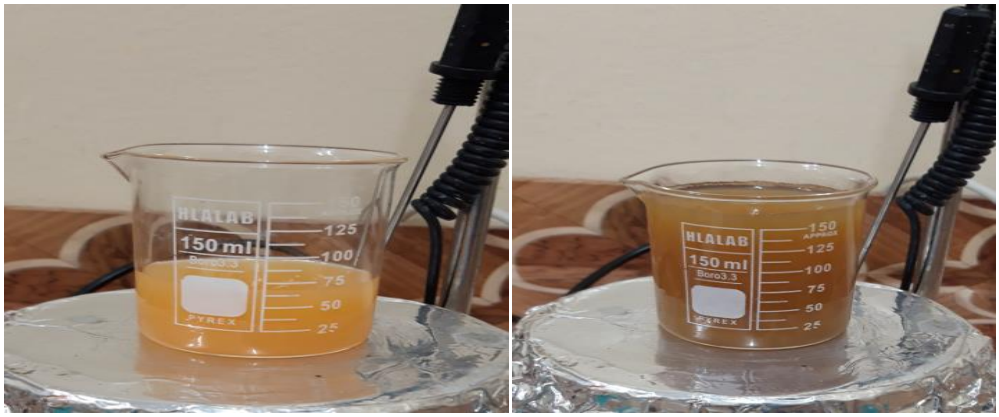
Fresh fruits of Iranian origin were bought from the markets, washed with water and distilled water several times, peeled and dried in an 40 ° C oven. They were grinded with an electric grinder and a soft powder of kaki peels was obtained. The powder (15 gm) was mixed completely with 200 ml of boiled distilled water and then homogenized on a magnetic stirrer. The final product solution was extracted by centrifugation at 4000 rpm for 25 min, and thereafter kept at 4°C untill use [16] .

Synthesis of MgO NPs by hot aqueous extract of the *Persimmon* peels

An aliquot of 40 ml aqueous extracts from the peels of *Persimmon* (P.P) was heated at 60 ° C on a magnetic stirrer, then 0.1 M (40 ml) of magnesium Nitrate Mg(NO3)2.6H2O was added and kept on stirring condition at 1500 rpm. After reaching the required temperature, 2M NaOH solution was added drop-wise into the reaction mixture to achieve a pH between 10-12. A solution of $Mg(OH)_2$ was formed after adding the alkaline solution and left for 2hr until its color changed to a brown color, as shown in Figure-1. The solution was then centrifuged at 4000 rpm for 15min. The precipitate was

placed in the oven at 400° C for 3hr. A white powder was obtained and collected carefully, as shown in Figure-2, then kept for characterization purposes. .

.



(a) (b)

Figure 1-Magnesium oxide nanoparticles by green method.(a) before adding NaOH (b) after adding NaOH.



Figure 2-Magnesium oxide nanoparticles powder by green synthesis.

The synthesized MgO NPs (0.1mg) was mixed with 100 ml of distilled water and processed in an ultrasonic processor device at 750 Watt and 20 kHz .The device operated for 5 days with 1and a half hours a day (10: 5 seconds of working: resting cycles).

The synthesized MgO nanoparticles and the reduced grain size of MgO NPS were characterized by X-ray diffraction (XRD), UV–visible spectroscopy, atomic force microscopy (AFM), field emission scanning electron microscopy (FESEM) and energy dispersive x-ray analysis (EDX).

Antibacterial activity of MgO nanoparticles

Preparation of bacterial culture solution

Two previously-identified bacterial strains (*Staphylococcus aureus* and *Escherichia coli*) were obtained from Biology department – College of Science /University of Baghdad. Each strain was subculturted in nutrient broth and incubated for 18 hr. at 37 °C, and then used as a bacterial stock solution for further experiments.

Minimal Inhibitory Concentration (MIC)

Antibacterial activity of MgO NPs was examined against pathogenic bacteria *S. aureus* (Gram-positive) and *E. coli* (Gram negative) using MIC examination in a microtiter polysteren plate with 96 flat bottomed wells. The freshly bacterial subcultures were prepared before starting the experiment by inoculating the bacteria in a 10 ml nutrient broth test tube and incubated for 18 hr. at 37 C̊. Different concentration of MgO NPs (250, 500, 1000, and 2000 µg/ml) were used and 100 µl of each MgO NPs concentration was mixed with 100 µl bacterial growth (after adjusting its concentration to $1.5*10^8$

cell/ml, 0.5 MacFerland turbidity) in each well of the microtiter plate. The lowest concentration of MgO NPs that showed no detectable growth was determined as MIC. A volume of 100 µl was transferred from the bacterial culture at the MIC as well as the previous higher concentration and spread on sterile nutrient agar plates, which were then incubated at 37 Ċ for 24 hr. The lowest concentration of MgO NPs that killed 100% of the bacteria was determined as the Minimal Bactericidal Concentration (MBC) [17].

Resazurin microplate assay

The test was performed in a microtiter polysterene 96 well plate as described by Coban (2012)[18], using the broth microdilution method with modifications. Resazurin powder was dissolved in phosphate-buffered saline (PBS), pH 7.5, to a final concentration of 0.1 mg/ml. Vortex mixer was used to ensure that the powder was well-dissolved. Fifty microliters of nutrient broth was dispensed into the 1st to the 6th well in two rows, while 50 µl of each MgO NPs concentration was pipeted into the 1st to the 3rd well in two raws for the ultrasonic-treated MgO NPs and into the 4th to the 6th well in two raws for the ultrasonic-untreated MgO NPs. Five microliters of bacterial suspention (at 0.5 MacFerland turbidity standard with aproximately $1.5*10^8$ cell/ml bacterial concentration) was inoculated into each previous well (1st raw with *E coli* bacterial growth and 2nd raw with *S aureus* bacterial growth). The plate was then covered loosely to avoid dehydration of the well suspention and incubated aerobically at 35Ċ for 18hr. After incubation of the broth microdilution plate, 15 µl of the dye was added to each well and mixed using an electronic multichannel dispenser. The plates were incubated for an additional 75 min at 37 Ċ (Figure-10). The change in blue color into pink indicated live bacterial cells while the maintanence of the blue or purple color indicate thed inhibited or killed bacterial cells.

Results and discussion

X-ray Diffraction

The cubic crystal system of the synthesized MgO was confirmed by the XRD (Figure-3). The 2θ peak positions were well identified with the JCPDS NO: 00-045-0946. Also, the crystalline size was evaluated by the following Debye Scherrer'sformula

$D= 0.94\lambda/\beta \cos \theta$

The crystalline size values and structural parameters of MgO NP_s synthesized by the green method are shown in Table-1. The results agree with those of EL-Moslamy *et al*. (2018) and Balraj *et al*. (2018) [19, 20]. The calculated crystallite size of the MgO NPs shows that the nanoparticles were prepared in the quantum confinement system, as shown in Table-1. There were no impurities, while the extra peaks in the synthesized material and the sharp peaks specified that the material is purely crystalline in nature.

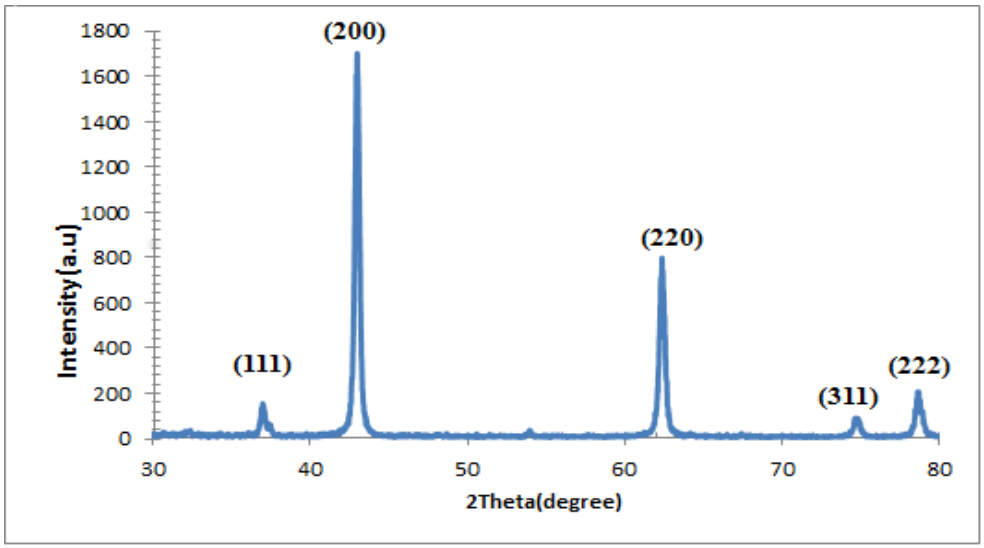


Figure 3-XRD patterns of MgO NPS powder.

Table 1-Crystalline size and structural parameters of MgO

2θ (Deg.)	**FWHM (Deg.)**	**Crystalline size D(nm)**	**Hkl**
37.001	0.0056	25.68	(111)
42.991	0.0058	25.62	(200)
62.363	0.0061	26.55	(220)
74.71	0.0059	29.23	(311)
78.65	0.0057	30.96	(222)

The optical absorption analysis

UV–VIS is the optic absorption spectrum [21]. The absorption spectra of the MgO were recorded within the wavelengths of 200-800. From Figure-4, it can be observed that , at absorbances of 240 nm and 310 nm, there were shifts towards the larger wavelength after treatment with the ultrasonic processor , leading to a decrease in the energy gap from 5.16 eV to 4. 0 eV. This result agrees withthat of Moorthy *et al*. (2015) and Sivalingam *et al*. (2012) [5, 22].

The energy band gaps of MgO NPs were calculed by the following formula

$E = hc/\lambda$

It was observed that the shift in the increasing wavelength leads to a decrease in the energy gap from 7.8 eV in the bulk MgO to 5.16 eV in the MgO NPs synthesized by the green method. This is possibly due to the increase in the aggregation of MgO NPs. This occurs because of defects that accompany the preparation of MgO NPs [9, 22].

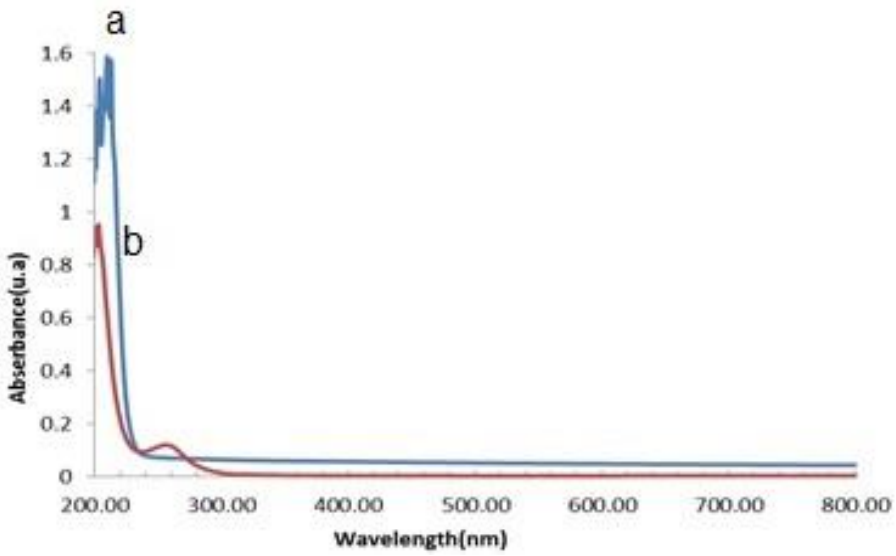


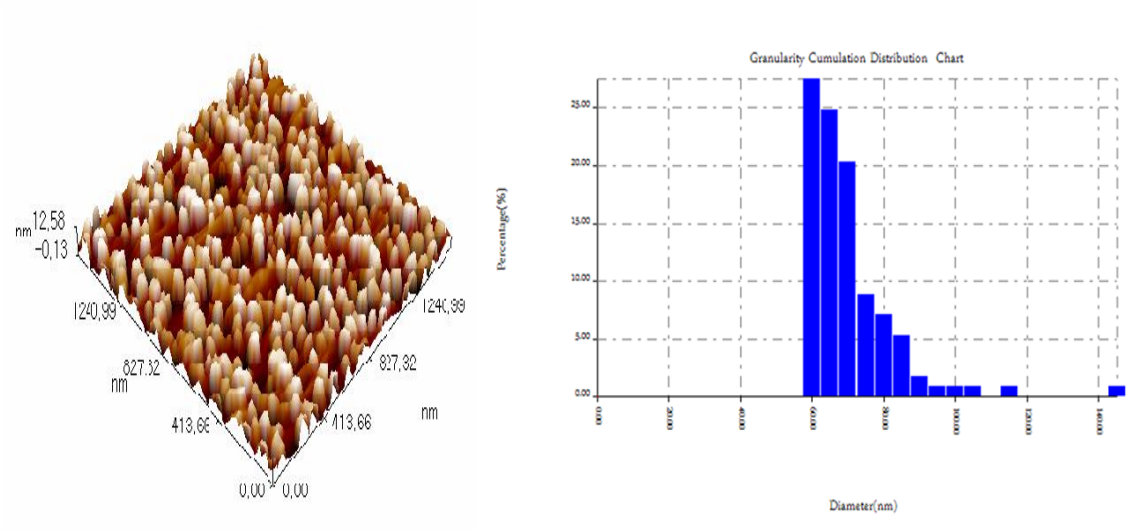
Figure 4-UV–Visible spectrum of MgO NPs (a) before treatment, (b)after treatment with ultrasonic waves.

Atomic Force Microscopy (AFM)

Atomic force microscopic examination allows identifying the plot topographies representing the surface elevation and the structure of the surface. This technique refers to digital images that allow quantitative measurements of surface features, such as root mean square roughness (Rq) , average roughness (Ra) and the analysis of images from different perspectives, including 3D simulation [23]. Figure-5 illustrates the three dimensional AFM images and granularity distribution of the MgO NPs synthesized by the green methods. It is important to note that the mean values were obtained and showed a statistical variance, depending on the location of the measurements performed on the samples. The average grain size for the MgO NPs was 67.73 nm, as show in Table-2, and It can be seen that the nanoparticles were approximately spherical.

Table 2-The information of the diameter in AFM analysis, volume %, and cumulation % of MgO nanoparticles

Avg. Diameter:67.73 nm			**<=10% Diameter:0 nm**					
<=50% Diameter:60.00 nm			**<=90% Diameter:80.00 nm**					
Diameter(nm)<	Volume (%)	Cumulation(%)	Diameter(nm)<	Volume (%)	Cumulation(%)	Diameter(nm)<	Volume (%)	Cumulation(%)
60.00	27.43	27.43	80.00	7.08	88.50	100.00	0.88	97.35
65.00	24.78	52.21	85.00	5.31	93.81	105.00	0.88	98.23
70.00	20.35	72.57	90.00	1.77	95.58	115.00	0.88	99.12
75.00	8.85	81.42	95.00	0.88	96.46	145.00	0.88	100.00



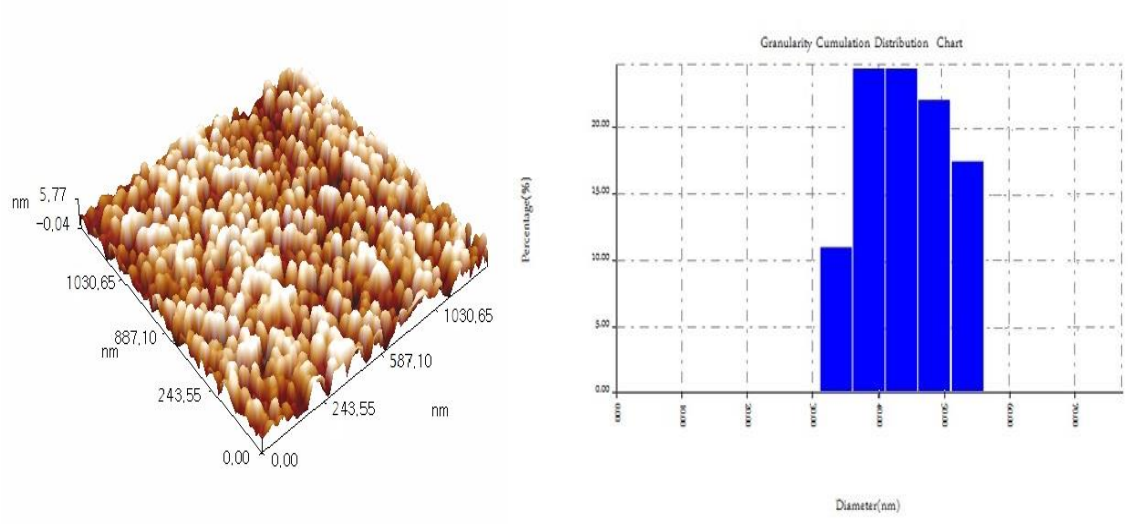
(a) **(b)**

Figure 5-AFM images before treatment with ultrasonic processor (a) three dimensions, and (b) histogram of the distribution of grain size.

Figure-6 clarifies the image of three dimension and the distribution of granularity accumulation of MgO NPs after treatment with thw ultrasonic processor. The average grain size of MgO NPs treated with ultrasonic processor was 42.33 nm, as show on Table-3 . It can be seen that the nanoparticles were approximately cylindrical. This result corresponds with that of the UV-Vis analysis.

Table 3-The information of diameter in AFM analysis, volume % and cumulation % of MgO nanoparticles after treatment with ultrasonic processor.

Avg. Diameter:42.33 nm			**<=10% Diameter:0 nm**					
<=50% Diameter:40.00 nm			**<=90% Diameter:45.00 nm**					
Diameter(nm)<	Volume (%)	Cumulation(%)	Diameter(nm)<	Volume (%)	Cumulation(%)	Diameter(nm)<	Volume (%)	Cumulation(%)
43.00	10.52	5.52	44.00	12.34	40.19	38.00	8.76	40.00
40.00	12.34	27.85	45.00	11.04	43.23			

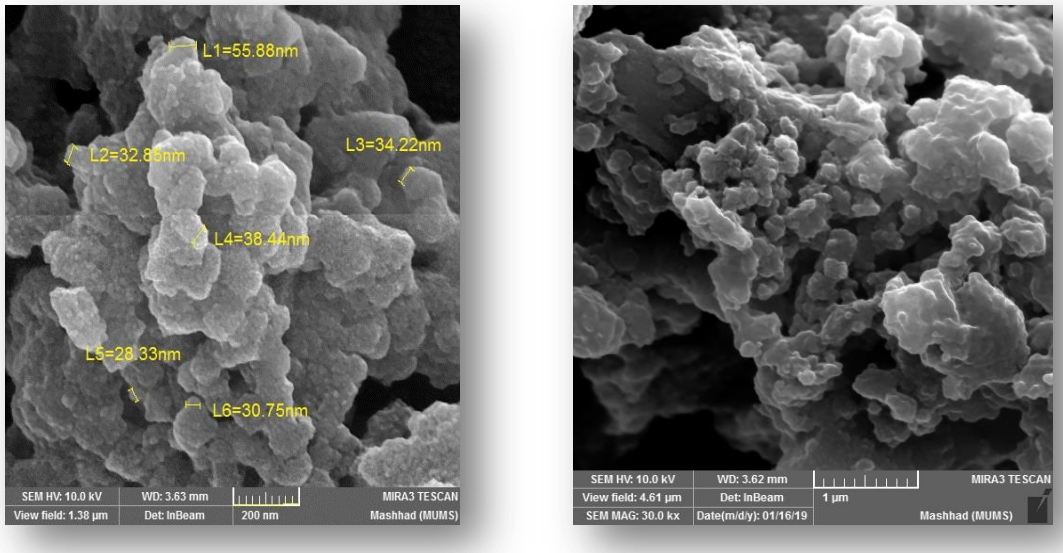


(a) (b)

Figure 6-AFM images after treatment with ultrasonic processor (a) three dimensions, and (b) histogram of the distribution of grain size.

Field Emission Scanning Electron microscopy (FE-SEM)

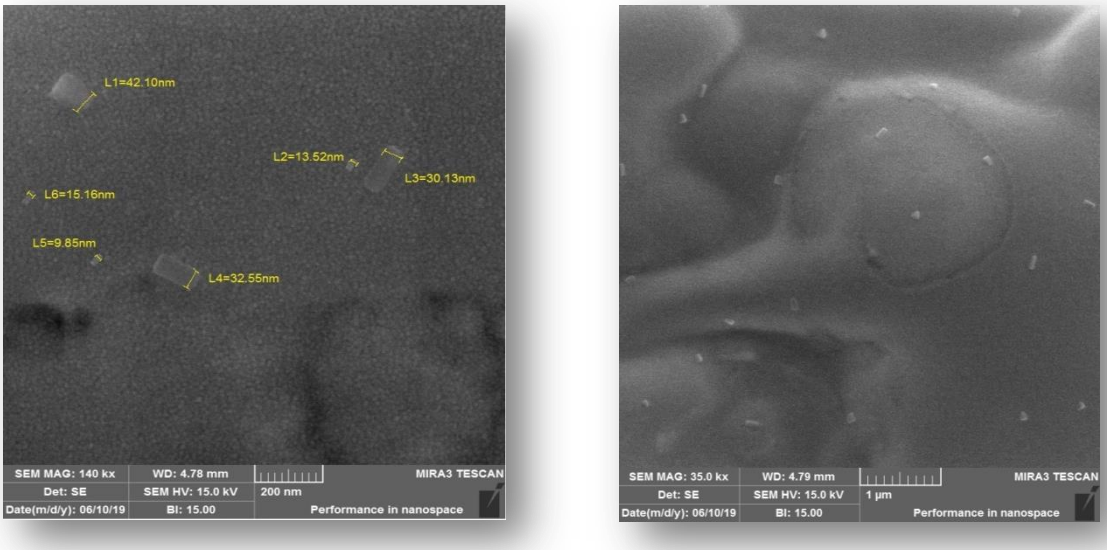
Figure-7 shows the surface morphology of MgO nanoparticles that were obtained using the FE-SEM image. By analyzing the image, it shows that the synthesized MgO NP_s were approximately spherical with an average diameter of 36.74 nm. In addition, they were aggregated and formed predominantly dense and irregular sharped flakes.



(a) (b)

Figure 7-The surface morphology of MgO NPs By FE-SEM (a) 200nm(b) 1µm.

The FESEM analysis for MgO NP_s with ultrasound effects was obtained as shown in Figure-8, with an average size of 23.88nm. There have been a noticeable change in the shape after using the ultrasonic mixer; the spherical shape was changed into cylindrical flakes with a homogeneous and almost uniform distribution for magnesium oxide nanoparticles .



(a) (b)

Figure 8-The surface morphology of $MgONP_s$ processed by ultrasonic, (a) 200nm (b)1µm.

EDX spectrum was recorded, as shown in Figure- 9 which shows a clear peak corresponding to Mg and O. Additional peaks of C , Si, Ca and Na were recorded. This result agrees with Hielscher, (2007) [16]. A strong peak was obtained at 1.1 keV to 1.3 keV for magnesium , while an oxygen peak was obtained around 0.2–0.4 keV. The observed strong peaks can be correlated to the formation mechanism to confirm the purity of the synthesized materials.

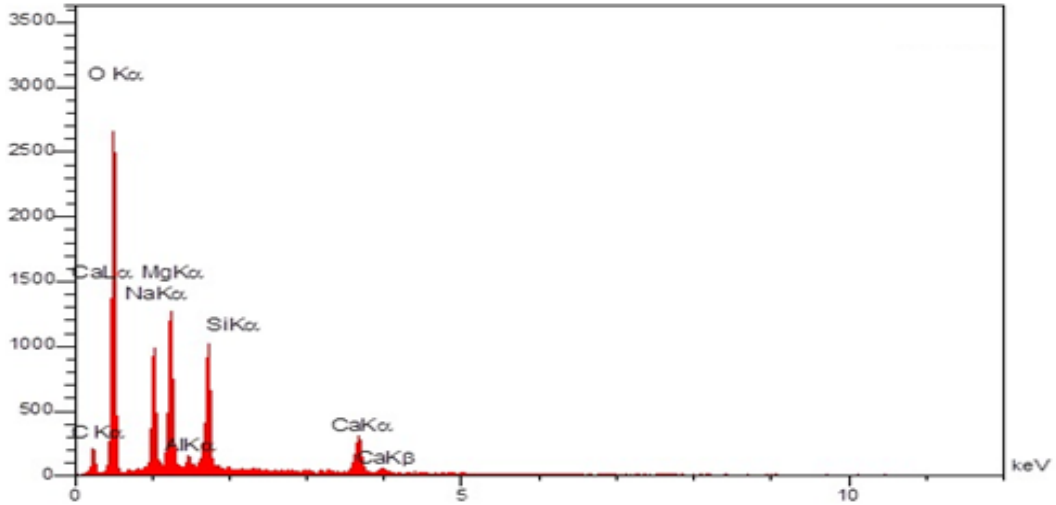


Figure 9-EDX analysis of the synthesized MgO nanoparticles.

Antibacterial activity of MgO nanoparticles

Antibacterial activity by MIC assay

The anibacterial activity of MgO NPs was detected against both *S.aureus* and *E.coli* pathogenic bacteria . The MIC value of MgO NPs against *E.coli* and *S.aureus* was 500 µg/ml with ultrasonic treatment. Whease the MgO NPs without ultrasonic treatment showed no effect against *E.coli*, although a higher concentration was used (2000 µg/ml)which showed the same MIC value against *S.aureus* at 500 µg/ml. The MgO NPs in general were previously shown to have antibacterial activities [24, 25]. Green synthesis of nanoparticles from this oxid metal is superior to chemical syntheses in different ways [26]. In this study, we used the peels of *Persimmon* extract in the green synthesis of MgO NPs, which showed antibacterial activities especially against Gram positive bacteria (*S. aureus*). This may be explained by the differences in the cell wall of Gram positive and Gram negative bacteria

[27]. The presence of active oxygen, such as superoxide, on the surface of the synthesized MgO NPs may be one of the reasons behind the significant antibacterial activity by causing cell death related to the cell membrane damage [28]. The results also showed the positive effects of using ulrasonic treatment for the produced MgO NPs on inhibiting the growth of bacteria. This can be attributed to the ability of the ultrasonic treatment to maintain the nanoparticles flouting and dispresed in the suspension rather then being aggregated as a sediment with no effect. In other words, ultrasound disruption shows more energy and reach higher levels of powder fragmentation [29], which enhance the effects of the MgO NPs against the pathogenic bacteria that grow in the broth suspention.

Antibacterial activity by resazurin microdilution assay

Antibacterial activity by resazurin was used as a confirmatory assay (growth indicator) of the MIC assay. In the 250 µg/ml treated wells, viable bacterial cells were detected (pink color) for both *E .coli* and *S.aureus* after 75 min of incubation (Figure-10). After incubation with 500 µg/ml, nanoflakes the non-viable cells started to be detected (purple color) (Figure-10), whereas totally non-viable cells were seen (blue color) at 2000 and 1000 µg/ml-treated samples. Growth was highly inhibited when the bacterial cells were incubated with MgO NPs treated with ultrasonic processor at a concnetrattion of 1000 µg/ml nanoparticles. From this assay, it was observed that the population of dead cells was increased with the increase of concentration. Furthermore, very low viability/growth of *S. aureus* was seen after incubation with 500, 1000 and 2000µg/ml of MgO NPs compared to control and compared to *E.coli* where. It was also observed that the population of dead cells increased in the concentrations of 2000 and 1000 of MgO NPs treated with ultrasonic mixer. The data obtained is similar to MIC assay , which gives a good indication for the useful and simple use of resazurin in the detection of the antibacterial activity of different nanopartical materials since this assay was used in different other materials such as plant extracts and essential oils.

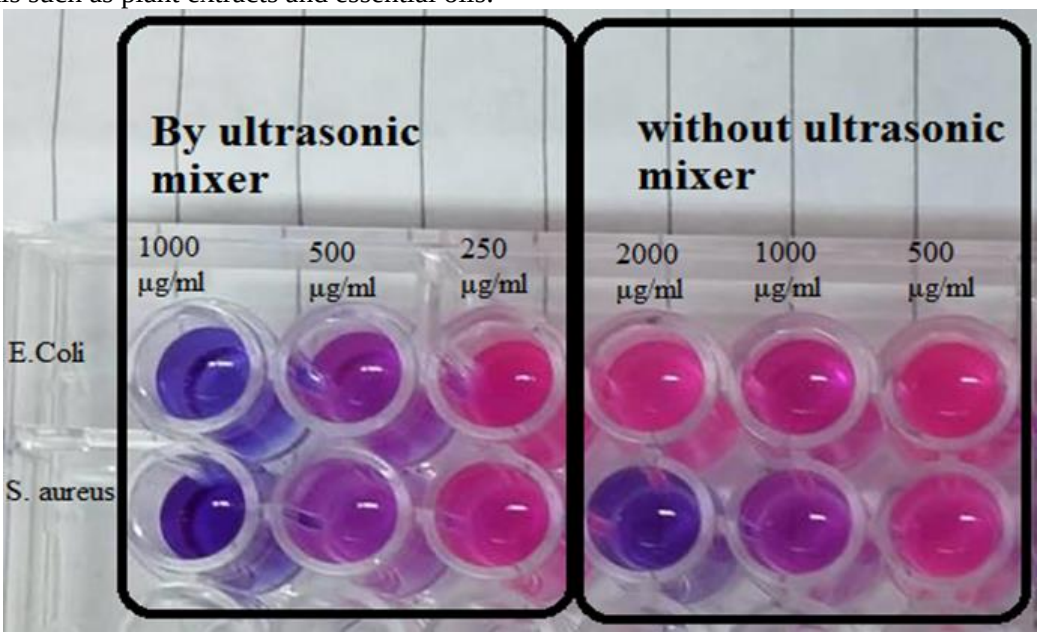


Figure 10-Plates after 75min. of modified resazurin assay. Pink color indicates growth and blue color means inhibition of growth.

Conclusion

This research is the result of biological synthesis and reduced particle size by ultrasonic treatment of MgO NPs and their ability to be applied as antibacterial agents. XRD confirms the molecular structure of MgO nanoparticles with a crystal size of 25.62 nm. Analyses of FESEM and AFM show the spherical nature of the MgO NPs prior to ultrasound processing. The effect of ultrasound reduced particle size and changed their shape from spherical to cylindrical. MgO Nps showed a minimum inhibitory concentration (MIC) at 500 µg / ml with a better effect for the ultrasound-treated sample.

References

1. Abe, J. **2018.** Self-Standing Carbon Nanofiber and SnO_2 Nanorod Composite as a High-Capacity and High-Rate-Capability Anode for Lithium-Ion Batteries. *ACS Applied Nano Materials*, **1**(6): 2982-2989.
2. Kaviyarasu, K. **2017.** In vitro cytotoxicity effect and antibacterial performance of human lung epithelial cells A549 activity of zinc oxide doped TiO2 nanocrystals: investigation of bio-medical application by chemical method. *Materials Science and Engineering*: C, **74**: 325-333.
3. Fukushi, D. **2017.** Decomposition of gas-phase organic pollutants over nanocrystalline tungsten oxide photocatalysts under visible-light irradiation. *Bulletin of the Chemical Society of Japan*, **90**(8): 885-892.
4. Kairdolf, B.A., X. Qian, and Nie, S. **2017.** Bioconjugated nanoparticles for biosensing, in vivo imaging, and medical diagnostics. *Analytical chemistry*, 2017. **89**(2): 1015-1031.
5. Moorthy, S.K. **2015.** Synthesis and characterization of MgO nanoparticles by Neem leaves through green method. *Materials Today: Proceedings*, **2**(9): 4360-4368.
6. Khalaf, S.A. and Ali, I.M. **2018.** Enhancement the Sensitivity of Zinc Sulfide Nanostructure Against NO2 Toxic Gas by Loading Graphene. *Iraqi Journal of Science*, **59**(4C): 2242-2248.
7. Wani, A. and Shah, M. **2012.** A unique and profound effect of MgO and ZnO nanoparticles on some plant pathogenic fungi. *Journal of Applied Pharmaceutical Science*, **2**(3): p. 4.
8. Mirzaei, H. and Davoodnia, A. **2012**. Microwave assisted sol-gel synthesis of MgO nanoparticles and their catalytic activity in the synthesis of hantzsch 1, 4-dihydropyridines. *Chinese journal of catalysis*, **33**(9-10): p. 1502-1507.
9. AL-Awadi, S.S., Shbeeb, R.T. and Chiad, B.T. **2018.** Effect of Silver Nanoparticles on Fluorescence Spectra of C480 dye. *Iraqi Journal of Science*, p. 502-509.
10. Leung, Y.H. **2014.** Mechanisms of antibacterial activity of MgO: non-ROS mediated toxicity of MgO nanoparticles towards Escherichia coli. *Small*, **10**(6): 1171-1183.
11. Sundrarajan, M., Suresh, J. and Gandhi, R.R. **2012**. A comparative study on antibacterial properties of MgO nanoparticles prepared under different calcination temperature. *Digest journal of nanomaterials and biostructures*, 2012. **7**(3): 983-989.
12. Mallavadhani, U., Panda, A.K. and Rao, Y. **1998.** Review article number 134 pharmacology and chemotaxonomy of diospyros. *Phytochemistry*, **49**(4): 901-951.
13. VARGA, A. and MOLNAR, J. **2000**. BiOIOgical Activity Of FeijOa Peel EXtractS. *Anticancer research*, **20**: 4323-4330.
14. Kuldiloke, J. **2002.** Effect of ultrasound, temperature and pressure treatments on enzyme activity and quality indicators of fruit and vegetable juices. Msc Thesis, von der Fakultät III – Prozeßwissenschaften – Institut für Lebensmitteltechnologie Lebensmittelbiotechnologie und – prozeßtechnik der Technischen Universität Berlin Msc Thesis,
15. Hielscher, T. **2007.** Ultrasonic production of nano-size dispersions and emulsions. arXiv preprint arXiv:0708.1831.
16. Das, B. **2018.** Biosynthesis of magnesium oxide (MgO) nanoflakes by using leaf extract of Bauhinia purpurea and evaluation of its antibacterial property against Staphylococcus aureus. *Materials Science and Engineering: C*, **91**: 436-444.
17. Janthima, R., Khamhaengpol, A. and Siri, S. **2018**. Egg extract of apple snail for eco-friendly synthesis of silver nanoparticles and their antibacterial activity. *Artificial cells, nanomedicine, and biotechnology*, **46**(2): 361-367.
18. Coban, A.Y. **2012**. Rapid determination of methicillin resistance among Staphylococcus aureus clinical isolates by colorimetric methods. *Journal of clinical microbiology*, **50**(7): 2191-2193.
19. EL-Moslamy, S.H. **2018**. Bioprocessing strategies for cost-effective large-scale biogenic synthesis of nano-MgO from endophytic Streptomyces coelicolor strain E72 as an anti-multidrug-resistant pathogens agent. *Scientific reports*, **8**(1): 3820.
20. Balraj, B. **2018**. Characterization, antibacterial, anti-arthritic and in-vitro cytotoxic potentials of biosynthesized Magnesium Oxide nanomaterial. *Materials Science and Engineering: B*, **231**: 121-127.
21. Smitha, S. **2008.** Studies on surface plasmon resonance and photoluminescence of silver nanoparticles. *Spectrochimica Acta Part A: Molecular and Biomolecular Spectroscopy*, **71**(1): 186-190.

22. Sivalingam, P. **2012.** Mangrove Streptomyces sp. BDUKAS10 as nanofactory for fabrication of bactericidal silver nanoparticles. *Colloids and Surfaces B: Biointerfaces*, **98**: 12-17.
23. Al-Rasoul, K.T., Abbas, N.K. and Shanan, Z.J. **2013**. Structural and optical characterization of Cu and Ni doped ZnS nanoparticles. *Int. J. Electrochem. Sci*, 2013. **8**(4): 5594-5604.
24. Tabassum, A., Sunita, D. and Raj, M.S. **2014.** Antibacterial effect of magnesium oxide nanoparticle on water contaminated with E. coli. *Res Rev J Microbiol Biotechnol*, **3**: 10-13.
25. Suresh, J. **2013.** Synthesis of Magnesium Oxide nanoparticles by wet chemical method and its antibacterial activity. in Advanced materials research. *Trans Tech Publ*.
26. Palanisamy, G. and Pazhanivel, T. **2017**. Green synthesis of MgO nanoparticles for antibacterial activity. *International Research Journal of Engineering and Technology*, 2017. **4**(9): 137-141.
27. Rao, K.G. **2014**. Structural properties of MgO nanoparticles: synthesized by co-precipitation technique. *International Journal of Science and Research*, **8**: 43-46.
28. Vatsha, B. **2013.** Effects of precipitation temperature on nanoparticle surface area and antibacterial behaviour of Mg (OH) 2 and MgO nanoparticles. *Journal of Biomaterials and Nanobiotechnology*, **4**(04): 365.
29. Taurozzi, J.S., V.A. Hackley, and Wiesner, M.R. **2011**. Ultrasonic dispersion of nanoparticles for environmental, health and safety assessment–issues and recommendations. *Nanotoxicology*, **5**(4): 711-729.